



# Treatment of osteoarthritis by implantation of Mg- and WE43-cylinders - A preclinical study on bone and cartilage changes and their influence on pain sensation in rabbits

Nina Angrisani<sup>a,\*</sup>, Christin von der Ahe<sup>a</sup>, Regine Willumeit-Römer<sup>b</sup>, Henning Windhagen<sup>a</sup>, Verena Scheper<sup>c</sup>, Michael Schwarze<sup>d</sup>, Björn Wiese<sup>b</sup>, Heike Helmholz<sup>b</sup>, Janin Reifenrath<sup>a</sup>

<sup>a</sup> Hannover Medical School, Clinic for Orthopaedic Surgery, Lower Saxony Centre for Biomedical Engineering, Implant Research and Development (NIFE), Hannover, Lower Saxony, Germany

<sup>b</sup> Helmholtz-Zentrum Hereon, Institute of Metallic Biomaterials, Geesthacht, Germany

<sup>c</sup> Hannover Medical School, Department of Otolaryngology, Lower Saxony Centre for Biomedical Engineering, Implant Research and Development (NIFE), Hannover, Lower Saxony, Germany

<sup>d</sup> Hannover Medical School, Clinic for Orthopaedic Surgery, Laboratory for Biomechanics and Biomaterials, Hannover, Lower Saxony, Germany

## ARTICLE INFO

### Keywords:

Magnesium  
Subchondral bone  
*In vivo*  
Gait analysis  
 $\mu$ -computed tomography  
CD271

## ABSTRACT

With its main features of cartilage degeneration, subchondral bone sclerosis and osteophyte formation, osteoarthritis represents a multifactorial disease with no effective treatment options. As biomechanical shift in the trabecular network may be a driver for further cartilage degeneration, bone enhancement could possibly delay OA progression. Magnesium is known to be osteoconductive and already showed positive effects in OA models. We aimed to use magnesium cylinders to enhance subchondral bone quality, condition of cartilage and pain sensation compared to sole drilling *in vivo*. After eight weeks of implantation in rabbits, significant increase in subchondral bone volume and trabecular thickness with constant bone mineral density was found indicating favored biomechanics. As representative for pain, a higher number of CD271+ vessels were present in control samples without magnesium. However, this result could not be confirmed by sensitive, objective lameness evaluation using a pressure sensing mat and no positive effect could be shown on either cartilage degeneration evaluated by OARSI score nor the presence of regenerative cells in CD271-stained samples. The presented results show a relevant impact of implanted magnesium on key structures in OA pain with missing clinical relevance regarding pain. Further studies with shifted focus should examine additional structures as joint capsule or osteophytes.

## Abbreviations

ACLT	Anterior cruciate ligament transection
BD	Bone mineral density
BV	bone volume
CD271	Cluster of differentiation 271
MSC	Mesenchymal stem cells
OA	Osteoarthritis
WE	Yttrium (W)-rare earths (E) containing alloy
Tr.th.	Trabecular thickness
$\mu$ CT	$\mu$ -computed tomography

## 1. Introduction

Osteoarthritis (OA) is the most common form of joint disease in the Western World today. During the last three decades, the total number of patients with OA increased by 132.2% and is expected to reach around 1 billion cases in 2050 [1]. These numbers face the current lack of availability of disease-modifying treatments [2], which adds to the high personal and economic burden; 2.2% of the total global years lived with disability (YLD) are attributed to OA [1,3]. Although long-time the

Peer review under responsibility of KeAi Communications Co., Ltd.

\* Corresponding author. Hannover Medical School, Clinic for Orthopaedic Surgery, Lower Saxony Centre for Biomedical Engineering, Implant Research and Development (NIFE), Stadtfeldamm 34, 30625 Hannover, Germany.

E-mail address: [angrisani.nina@mh-hannover.de](mailto:angrisani.nina@mh-hannover.de) (N. Angrisani).

<https://doi.org/10.1016/j.bioactmat.2024.06.003>

Received 23 November 2023; Received in revised form 20 April 2024; Accepted 1 June 2024

2452-199X/© 2024 The Authors. Publishing services by Elsevier B.V. on behalf of KeAi Communications Co. Ltd. This is an open access article under the CC BY-NC-ND license (<http://creativecommons.org/licenses/by-nc-nd/4.0/>).

degradation of the joint cartilage was considered the predominant pathology and driver for OA progression, recently the multifactorial character of this disease has been identified and moved to the focus of research including all adjacent structures as subchondral bone, joint capsule and synovium, menisci, nerves, ligaments and peri-articular muscles [4]. In 2019, the knee was the most frequently affected joint accounting for more than 60 % of the total prevalent cases [5]. Due to the discordance between radiographic findings and pain symptoms in knee OA [6], it is important to unveil the underlying mechanisms for OA pain to develop effective treatment options and therewith lower the patients' burden. Characteristics of OA are progressive cartilage loss, subchondral bone remodelling and sclerosis, osteophyte formation and synovial inflammation, all contributing to pain and increasing disability [7,8]. The burning pain described by OA patients is characteristic to be mediated by fine unmyelinated nerve fibres, which are most commonly perivascular [9]. In dependence of their content of neuropeptides they can be classified as sensory or sympathetic and the presence of these nerves has been reported in osteophytes, subchondral bone marrow and vascular channels leading from subchondral bone into the articular cartilage of different species supporting the role of subchondral bone contribution to pain in OA [9].

Magnesium (Mg) and Mg alloys turned up as potential osteosynthesis materials in the early 2000s and were examined in a plethora of *in vitro* and *in vivo* studies [10]. The rationale for using alloys as e.g. WE43 is the enhancement of biomechanical properties [11] while corrosion rate is similar or only slightly elevated in comparison to pure Mg [12]. Although their use as bone fixation devices for long bones could not be realized so far due to mechanical deficits [13], particularly different types of screws were successfully tested [14–16] and several entered routine clinical use. Approved and commercially available implants are either Mg–Zn–Ca-based (currently Innosys Corp., South Korea, and Bioretac, Finland) or WE43 based (currently medical magnesium, Germany, Biotronik, Switzerland, Syntellix, Germany). On account of their proven general biocompatibility and their osteoconductive properties (support of tissue ingrowth, osteoprogenitor cell growth, and development for bone formation) [17,18] Mg and Mg alloys are subjects of many different studies until now [19–21]. Apart from its effects on bone metabolism and fracture healing there is growing evidence of its possible beneficial role in OA, which is summarized by Kuang et al. [22]. Among others, Mg could induce osteogenic differentiation of mesenchymal stem cells (MSCs) [17], osteoblast activity [23] and enhance the proliferation and re-differentiation of chondrocytes, however with regard to an upper limit for reversion of this effect [24]. Yao et al. could show a decreasing effect of Mg ions in combination with vitamin C application on OA *in vivo* in mice [25]. The aim of a pilot study performed in our research group with rabbits was to use the osteoconductive capacity of Mg to increase the subchondral bone quality and therewith enhance the condition of articular cartilage inside the osteoarthritic knee by implanting small Mg cylinders [26]. While a significant increase in bone volume and trabecular thickness with simultaneous unchanged bone mineral density resulted from the implanted Mg, there was no differences between the Mg and the control group regarding cartilage degeneration of the operated knee and lameness, both evaluated by scores. However, the condition of the cartilage of the contralateral, non-operated knee was significantly worse in the control group [26]. This led to the hypothesis that the implanted Mg cylinders might reduce pain on a level that could not be detected by the applied, rather insensitive score. Furthermore, as it was a pilot study, the number of animals was relatively low. Therefore, the study presented here aimed to reassess the results in a larger cohort using the same set up while deepening the evaluation methods with focus on pain. We hypothesized that subchondrally implanted small Mg-based cylinders increase the bone volume and trabecular thickness with constant bone mineral density compared to sole drilling holes and lead to a better quality of articular cartilage in both knees also in this larger cohort. To address pain we implemented an objective lameness evaluation using a pressure

sensor mat and added immunohistochemical evaluation for the detection of nerve related structures. As WE43 and WE43 based alloys have already been approved for clinical use, we included an additional group, which received WE43 cylinders to assess the influence of the alloying components.

## 2. Material and methods

### 2.1. Cylinder

For the present study, cylindrical implants were made from two different base materials, pure Mg [26] and a WE43 like Mg alloy. The pure Mg were produced as described in Ref. [26]. For the WE43 wire pure magnesium (Mg) (99.985 %, MAGONTEC, Sydney, Australia) was melted and 4 wt% of Yttrium (Y) (99 %, Stanford Advanced Materials, Birtcher, USA) and 3 wt% of Gadolinium (Gd) (99.9 %, Dr. Ihme GmbH, Berlin, Germany) were added in to the molten Mg. This Mg–4Y–3Gd melt was stirred for 10 min and was casted with the permanent direct chill casting process. The ingot was machined into cylinders with a diameter of 49 mm and a length of 150 mm for the direct extrusion process. The pure Mg was melted without any further additions, cast, and processed into billet like the WE43. The cast WE43 ingots were solution annealed for 8 h at 525 °C and quenched in water. Prior to the extrusion at 350 °C for pure Mg and at 450 °C for WE43, the billets were preheated for 1 h. The extrusion was carried out at an extrusion speed of 0.11 mm/s for pure Mg and 0.2 mm/s for WE43 and using a die with four holes of 0.8 mm for pure Mg and Ø1.0 mm for WE43 each. Cold wire drawing on WE43 wire was carried out with a drawing die in steps of 0.92, 0.82, 0.73, 0.65, 0.58, 0.52 and 0.50 mm. The recrystallization annealing was conducted for 5 min at 400 °C per step until the final diameter of 0.5 mm was obtained. For pure Mg, the drawing die was used in steps of 0.73, 0.65, 0.58, 0.52 and 0.50 mm with annealing at 350 °C for 5 min. Both wires were drawn at a speed of 0.25 mm/s. The final alloy concentration is shown in Table 1. Fig. 1 displays an exemplary picture of the microstructure of WE43 cylinders. An optical microscope (Leica Wild M3Z) was used to determine the exact metrics of  $n = 26$  cylinders, which had an average length and diameter of  $957.5 \pm 5.5$  and  $519.5 \pm 2.5$   $\mu\text{m}$ . The cylinders were cleaned in an ultrasonic bath with n-hexane (20 min), acetone (20 min) and 100 % ethanol (3 min) [25]. Subsequently, a first sterilization was performed in 70 % ethanol. Cleaning was performed according to an internal standard and is identical to that used in the pilot study in Ref. [24]. Prior to *in vivo* implantation, cylinders were sterilized using gamma-radiation with Cobalt-60 at 32.2 kGy (BBF Sterilisationsservice GmbH, Kernen, Germany).

### 2.2. Housing and Handling

The *in vivo* experiments were performed according to the German Animal Welfare act after approval by the LAVES (Lower Saxony State Office for Consumer Protection and Food Safety under registration number 33.9-42502-04-18/2774) including 36 female New Zealand White rabbits (Charles River Laboratories, Research Models and Services GmbH, Germany) with an average bodyweight of  $3760 \pm 390$  g. They were housed in groups of 12 animals each under constant conditions (room temperature  $18 \pm 3$  °C, humidity  $55 \pm 10$  %) allowing free movement. Enrichment was implemented by different types of hiding places (wooden or card boxes), providing of platforms, hay (freely and in balls) and fresh food like carrots, cucumber, lettuce and sweet peppers.

**Table 1**

Chemical composition of the materials, measured on the bulk material; not detected (n.d.). wt%: weight percent; ppm: parts per million.

	Y [wt%]	Gd [wt%]	Fe [mg/kg]	Cu [mg/kg]	Ni [mg/kg]
Mg	–	–	$20 \pm 2$	$15 \pm 1$	$13 \pm 2$
WE43	$3.53 \pm 0.65$	$2.52 \pm 0.10$	$50 \pm 4$	$5 \pm 1$	n.d.

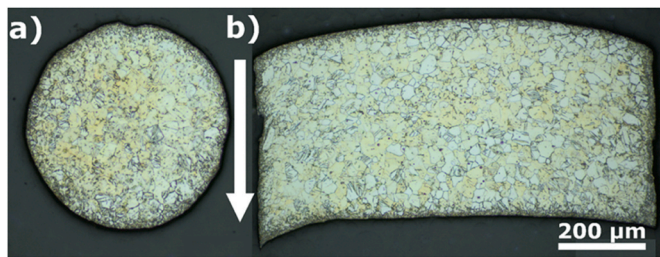


**Fig. 1.** Micrographs of (a) transversal and (b) longitudinal direction of the WE43 cylinder. The arrow indicates the process direction of cutting, which was inverse to the punching direction. The scale bar is valid for both micrographs. For micrographs of transversal and longitudinal direction of Mg cylinders, please see Ref. [26].

### 2.3. Surgery

The surgical intervention for the development of post-traumatic OA and the subsequent implantation of Mg cylinders are described in detail by Ref. [26]. In brief, at the age of  $\geq 24$  weeks, the rabbits underwent an anterior cruciate ligament transection (ACLT) of the right knee, including an incision of the medial meniscus. For the second surgery after development of OA 12 weeks later, rabbits were randomly assigned to three groups ( $n = 12$  each) by weight and grade of lameness, so that the mean of both was similar in each group. The animals received 20 drill holes, five each in the lateral and medial compartment of the femur condyles and tibia plateaus. While group 1 and 2 received one Mg or WE43 cylinder, respectively, per drill hole (“Mg group” and “WE group”), animals of group 3 got drill holes only and served as control group (“Drilling group”). Afterwards, joint instability was fixed by an extracapsular fixation [27]. Anaesthesia, peri- and postsurgical medication was similar for both surgeries [26]. Eight weeks after the second surgery, animals were euthanized using an intracardially injected pentobarbital overdose (800–900 mg/animal, Narkodorm®, CP-Pharma) during deep anaesthesia.

### 2.4. Clinical assessment

During the eight weeks follow up, weight, general condition, spontaneous behaviour and wound healing progress were assessed by a score scheme ranging from 0 (normal condition/no changes) to 20 (severe changes). According to the pilot study [26] score was also used to evaluate pain including analysis during orthopaedic examination (“passive pain”) and during free motion of the animals in their stable (“active pain”).

### 2.5. Gait analysis

For the refinement of lameness analysis and to detect even slight differences in the gait, load bearing was analyzed using a pressure sensor mat (model *pliance*® S2065, Novel GmbH, Munich, Germany). The detailed set up and calculation is published by von der Ahe et al. [28]. After the establishment of the physiological range preoperatively, post-operative measurements were performed once a week. On measurement days, small groups of rabbits including two to four animals were placed in the experimental set up and motivated to move over the sensor mat individually. Each run was filmed simultaneously using a web cam. For the calculation, five runs of each rabbit per measurement day were recorded. The parameter measured was the integral of force over time during contact by the associated hind paw. A symmetry Index was calculated ( $I = (x_{\text{right}} - x_{\text{left}}) / (x_{\text{right}} + x_{\text{left}})$ ) based on Robinson et al. [29] and the ratio was named *ratio<sub>force</sub>*. Values  $< 0$  show a higher load bearing of the left, non-operated limb, while values  $> 0$  show a higher load bearing of the right, operated limb.

### 2.6. Changes in subchondral bone

To detect quantitative changes of the subchondral bone  $\mu$ -computed tomographic ( $\mu$ CT) scans (XtremeCTII, ScancoMedical AG) were performed immediately after implantation of the cylinders/drilling of holes as well as four and eight weeks later. Scanning parameters were set to 353 mAS, 42.7 mGy at an integration time of 103 ms. Voxel size was 30  $\mu$ m. Volume of interest was defined for both femoral condyles, which included the subchondral bone plate and the underlying trabecular bone around the cylinders. For evaluation, grey value thresholds were set to 160 (lower threshold) and 255 (upper threshold). Changes over time in bone volume (BV), trabecular thickness (tr.th.) and bone mineral density (BD) of both femoral condyles were evaluated using IPL software (ScancoMedical AG). BD was expressed as milligram hydroxyapatite per cubic centimeters (mg HA/ccm). For exact evaluation, regular calibration of the device is performed using five standardized HA rods. Calculation procedure is described in detail by Ref. [26].

To evaluate the influence of the cylinder on cellular reactions regarding bone volume, histological samples were prepared and analyzed. Therefore, following euthanasia and macroscopic evaluation of the cartilage (see below), condyles were separated using a band saw and fixed in 4 % neutral buffered formalin for at least one week. Subsequently, the bone parts were embedded in Technovit 9100 New according to the manufacturer’s protocol (Kulzer GmbH, Hanau, Germany). Thin sections of 4  $\mu$ m were prepared using a hard tissue rotation microtome (Leica RM2255, Nussloch, Germany) and dried. Slides were stained for osteoclasts using tartrate-resistant acid phosphatase staining. After de-plastisation in Xylol ( $4 \times 5$  min, Carl Roth, Karlsruhe, Germany) and (2-Methoxyethyl)-acetat (60 min, Carl Roth, Karlsruhe, Germany), tissue was re-hydrated in a descending alcohol series (Carl Roth, Karlsruhe, Germany, 2x Isopropanol, 1  $\times$  96 % Propanol, 1  $\times$  70 % Propanol, 1x de-ionized water, 2 min each) and afterwards treated with 0.2 M Acetate buffer for 20 min. Staining was performed in staining solution comprising of Acetate buffer, Naphthol AS-MX Phosphate and Fast red for at least 90 min at 37 °C. After rinsing in de-ionized water, counter-staining was performed with Haemalum for 1 min followed by 10 min rinsing in running tap water.

The region of interest was defined as the double extend of the cylinder size, resulting in an area of  $1000 \times 2000 \mu$ m (Fig. 2). All regions of cylinder implantation site or drilling hole, respectively, were taken into account independent of whether there are two or one regions present. Of these possible differences between samples was taken account by calculating the number of osteoclasts per  $\text{mm}^2$  bone (OC/ $\text{mm}^2$ ) using Image J. Osteoclasts were counted by two different independent examiner, mean values were calculated and compared between the

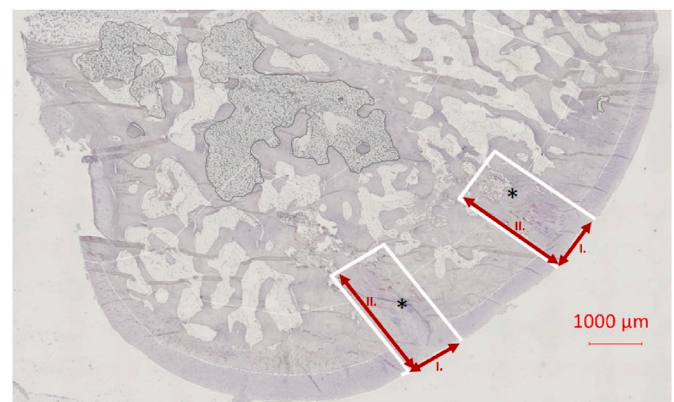


**Fig. 2.** Exemplary histologic TRAP-stained slice with scheme of the defined area for evaluation of osteoclast quantity in the region of the magnesium cylinder and drill hole, respectively. \*: region evaluated for OC quantity. Distance I.: 1000  $\mu$ m. Distance II.: 2000  $\mu$ m.

groups.

### 2.7. Degradation of WE43 cylinders

Additionally, degradation rate of WE43 cylinders was evaluated using the  $\mu$ CT data acquired as described above. Therefore, contours for each cylinder on the day of implantation were set in the femur condyles and transferred to the eight week scan. Analogous to the changes in subchondral bone, volume, density and, additionally, surface area were calculated using a grey value threshold of 260. Mean values for all three parameters were calculated per animal and used for further calculation. Degradation rate was computed as  $CR = \Delta V/A \cdot t$  according to Witte et al. [30] with CR (corrosion rate),  $\Delta V$  (change in volume), A (surface area exposed to corrosion) and t (time of corrosion). Due to the similar grey value of Mg cylinders and bone, separation between both was not possible, so that no degradation rate could be calculated for Mg implants.

### 2.8. Changes of articular cartilage

After euthanasia, tissue around the knees was carefully removed, the knee joint of both limbs exposed and cartilage changes and presence of osteophytes assessed according to Laverty et al. [31] and described by Ref. [26]. The score for the cartilage evaluation ranged from 0 (“*surface smooth with normal cartilage*”) to 4 (“*regions of complete cartilage erosion with subchondral bone exposed*”). Osteophytes were rated according to their presence and severity from 0 (“*absent*”) to 4 (“*severe*”).

Afterwards, tissue samples were prepared, fixed and embedded as described above. Slides were stained with Safranin O/Fast Green. After de-plastisation in Xylol (4 × 5min) and (2-Methoxyethyl)-acetat (10 min), tissue was re-hydrated in a descending alcohol series (Carl Roth, Karlsruhe, Germany, 2x Isopropanol, 1 × 96 % Ethanol, 1 × 70 % Ethanol, 1x de-ionized water, 2min each). Then, samples were stained in Safranin O (Merck, Darmstadt, Germany) for 12 min, rinsed shortly in de-ionized water, followed by staining with Fast Green (Carl Roth, Karlsruhe, Germany) for 3 min. Slices were de-hydrated again in an ascending alcohol series and Xylol. Evaluation was carried out by the application of a semi quantitative score according to Ref. [31] which included staining intensity of the tissue, structure, chondrocyte density and cluster formation. The maximum summed score value that could be reached is 24.

Furthermore, CD271 staining using a low-affinity anti-nerval growth factor receptor antibody was performed. Therefore, slices were de-plastified and rehydrated using (2-Methoxyethyl)-acetat, xylol and Isopropanol in descending concentrations. All rinsing steps were performed using 0.05 M tris buffered saline. Proteinase K was applied for demasking of binding sites. As primary and secondary antibodies, mouse-*anti*-CD271 and goat-*anti*-mouse were used, respectively. Streptavidin x Cy3 served as detection system. Slides were covered using Roti-Mount FluorCare DAPI. See detailed protocol in the supplementary materials (Table S1).

One representative slice of each sample was used for analysis of the whole condyle area. A semiquantitative score was used for the evaluation of the CD271+ cells in the cartilage ranging from 0 (no cells) through 1 (single cells), 2 (multifocal appearance) and 3 (grouped multifocal appearance) up to 4 (large scale appearance in whole area). Furthermore, stain-positive vessels were counted using the same slices. Therefore, subchondral bone area was screened and CD271+ vessels were included in the calculation if they appeared in an area of approximately 200  $\mu$ m beneath the articular cartilage.

### 2.9. Statistical evaluation

Statistical analysis was performed using SPSS® version 27 (IBM® Deutschland GmbH, Ehningen, Germany). Mean values and standard deviation were determined for all metric parameters and the median for

ordinal data. Results were tested for normal distribution using Kolmogorov-Smirnov. Normal distributed, metric data between the groups were compared with one-way ANOVA, whereas not normal distributed and ordinal data were tested using Kruskal-Wallis and Friedman test. For the comparison of left and right knees within each group, t-test for paired samples were applied. Values of  $p < 0.05$  were considered significant.

Boxplots were produced using Excel 2016 (Microsoft Corporation, USA).

## 3. Results

As long as not stated otherwise, result data included 35 of 36 rabbits. One rabbit died in an anaesthetic accident during the  $\mu$ CT scan after the second surgery. In total, Mg and Drilling group included 12 animals while WE group included 11 animals.

### 3.1. Clinical assessment

Comparable to the pilot study, none of the animals showed an impairment of the general condition or the spontaneous behaviour after neither the first nor the second surgery. The mean weight of all rabbits at the second surgery was  $3891 \pm 355$  g (Mg:  $3893 \pm 458$  g, WE43:  $3895 \pm 270$  g, Drilling:  $3887 \pm 343$  g). After the second surgery the mean weight loss tended to be slightly lower in the WE group than in the Mg and Drilling group. However, the difference was statistically not significant.

Independent of the group assignment some animals showed mild problems in wound healing represented by prolonged mild swelling, redness and secretion most likely as reaction to the suture material.

Level and progression of passive and active pain scores were comparable to the pilot study [26]. Both scores showed no differences between the three groups and therefore those data are not illustrated in a respective figure. After drilling/implantation of the cylinders, animals were sensitive to the orthopaedic examination for eight to eleven days. Active pain score was higher after the second surgery with values up to 3 but again decreased earlier than after ACLT surgery; all animals were scored for normal load bearing after a maximum of 35 days post implantation surgery.

### 3.2. Gait analysis

On each measurement day, there were some animals, which did not reach five successful runs. The most common reason was that they hopped over or slowed down/stopped on the mat. After several repetitions, the motivation of the animals faded and they just remained sitting on the floor unwillingly to complete another run. In such situation and with respect to animal welfare, the minimum number of successful runs was set to three.

On one day before the second surgery, the pressure sensor mat was not available due to technical problems, so that 12 animals could not be evaluated in the week before drilling/implantation of the cylinders. Therefore, mean values stated are based on  $n = 24$  rabbits. Furthermore, there were few values for some measurement days, which could not be evaluated because individual sensors of different paws overlapped impeding the determination of a specific region of interest.

One week before drilling/implantation of the cylinders, the mean value of all animals was still slightly under the physiological range meaning that most animals loaded their non-operated limb slightly more than their operated limb (Fig. 3). In the first week after the surgery all groups showed a significant shift of load bearing to the non-operated side with no significant differences between the groups (Mg:  $-0.64 \pm 0.10$ ; WE43:  $-0.63 \pm 0.19$ ; Drilling:  $-0.64 \pm 0.20$ ). Up to week 3, animals of the WE group seem to recover slightly faster than Mg- and Drilling animals, approaching the physiological range earlier (week 3: Mg:  $-0.53 \pm 0.14$ ; WE:  $-0.38 \pm 0.21$ ; Drilling:  $-0.46 \pm 0.21$ ) (Fig. 3).

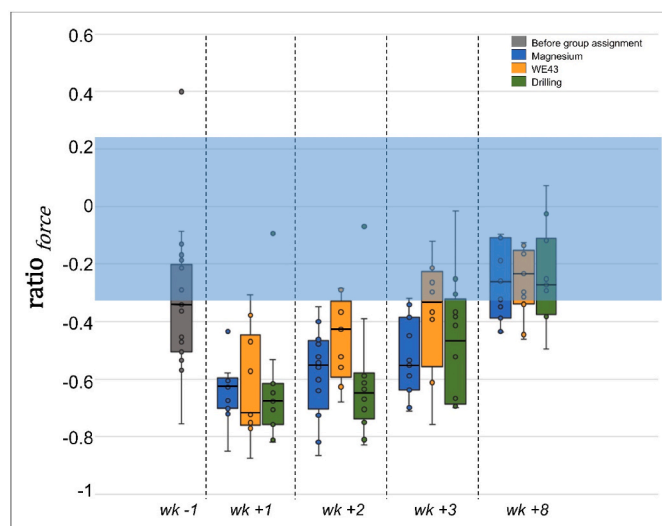


**Fig. 3.** Course of lameness one week before (grey boxplot) and in week +1, +2, +3 and +8 after drilling/drilling and cylinder implantation (coloured boxplots). Light blue: physiological range of weight levelling between right and left hind limb (0 represents even distribution of load). Dark blue: Magnesium group; orange: WE group; green: Drilling group. Number of animals included in the analysis for week -1: Mg/WE/Drilling n = 8; week +1: Mg n = 12, WE n = 10, Drilling n = 11; week +2: Mg n = 12, WE n = 10, Drilling n = 11; week +3: Mg n = 11, WE n = 8, Drilling n = 12; week +8: Mg n = 11, WE n = 11, Drilling n = 11.

However, this difference was not statistically significant. From week 4 onwards, the groups were in a similar range reaching the physiological range all three of them together in week 8 after implantation (Mg:  $-0.26 \pm 0.13$ ; WE43:  $-0.26 \pm 0.12$ ; Drilling:  $-0.24 \pm 0.17$ ).

### 3.3. Changes in subchondral bone

Six animals (one rabbit of the Mg, two rabbits of the WE group and three rabbits of the Drilling group) are not included in the evaluation due to different reasons (scan had to be aborted to shorten the anaesthetic period, animals moved slightly during scan procedure resulting in blurred data, bad positioning of the animal inside the scanner).

Significant differences were found for all parameters. During the first four weeks, increase in BV was higher than in the second four weeks. Overall after the eight weeks implantation period, BV was more than twice as high in the Mg group ( $33.93 \% \pm 11.37$ ) and nearly twice as high in the WE group ( $30.69 \% \pm 6.04$ ) compared to the Drilling group ( $15.84 \% \pm 7.71$ ) ( $p \leq 0.001$ , Fig. 4A).

For tr.th. the results were similar with a higher increase from implantation to week 4. The total percentage increase in tr.th. after eight weeks of implantation in both cylinders group was higher than in the drilling group ( $20.65 \pm 6.61 \%$ ), reaching values of  $40.31 \pm 11.27 \%$  and  $32.25 \pm 10.65 \%$  for Mg and WE, respectively. This difference was also highly statistically significant ( $p \leq 0.001$ ) (Fig. 4B).

The changes of BD in all groups were in a low range with slight increase in density over the whole implantation period. In the first four weeks, all three groups showed a slight decrease in density followed by clear however also small increase in the second four weeks. These changes sum up to a total of  $1.95 \% \pm 1.47$ ,  $0.57 \pm 1.84$  and  $0.08 \% \pm 1.91$  for Mg, WE and Drilling group, respectively. After eight weeks, highest percentage increase of BD was therewith found in animals of the Mg group (Fig. 4C).

### 3.4. Degradation of WE43 cylinders

A total of n = 90 cylinders were included into the calculation

resulting from n = 9 rabbits.

The mean total cylinder volume at implantation calculated by  $\mu$ CT was  $0.15 \pm 0.0 \text{ mm}^3$ , the mean surface area  $1.58 \pm 0.04 \text{ mm}^2$  and the mean density  $1740.73 \pm 4.97 \text{ mg HA/cm}^3$ . After eight weeks of implantation, the cylinders degraded substantially. The mean volume decreased by more than half to  $0.07 \text{ mm}^3$ . Also, the loss of surface area reached considerable 38.19 % to  $0.97 \text{ mm}^2$ . The loss in density was on a lower level, reaching 22.82 % ( $1342.79 \text{ mg HA/mm}^3$ ). All results are depicted in Fig. 4D.

Based on these values, degradation rate was calculated to be 0.33 mm/year.

### 3.5. Number of osteoclasts in the region of implanted cylinders

The number of samples which met the criteria for inclusion into the evaluation of OC number were n = 9 (Mg group), n = 7 (WE group) and n = 7 (Drilling group).

The differences in mean values between the groups were statistically significant ( $p = 0.047$ ). While both cylinder groups showed fewer OCs with no statistically significant results (Mg:  $2.64 \pm 3.35 \text{ OC/mm}^2$ ; WE43:  $3.17 \pm 4.05 \text{ OC/mm}^2$ ) the number of OC in the Drilling group was significantly higher ( $7.02 \pm 2.52 \text{ OC/mm}^2$ ,  $p(\text{Mg} - \text{Drilling}) = 0.02$ ;  $p(\text{WE43} - \text{Drilling}) = 0.047$ ) (Fig. 5).

### 3.6. Changes in cartilage

#### 3.6.1. Macroscopic changes

Except for one rabbit of the Mg group, which exhibited a very small arthritic lesion most lateral in the region of the sesamoid bone, all left, non-operated knees showed no macroscopic changes. The articular cartilage of the right femur and tibia showed pathological changes in all animals with no statistical differences between femur and tibia or between the groups (Fig. 6). The median values of the cartilage score for femur and tibia, respectively were 3.5 (min/max: 1/4) and 3.5 (min/max: 1/4) in the Mg group, 2.5 (min/max: 1/4) and 3.0 (min/max: 1/4) in the WE group and 2.75 (min/max: 1/4) and 2.75 (min/max: 1/4) in the Drilling group.

Similar to the cartilage results, there were no statistical differences between the groups regarding osteophyte formation. In all animals, they were predominantly situated proximal of the actual joint surface lateral and medial of the patellar sliding plane and reached overall severe shaping. Results and exemplary pictures are shown in Fig. 6. Median values (min/max values) for the groups were 3.0 (2/3) for Mg, 3.0 (2/3) for WE and 2.5 (2/3) for Drilling group, respectively.

#### 3.6.2. Histological changes

Histological evaluation of Safranin-O fast green stained slices could neither show any differences between right, operated cartilage nor the left, non-operated one. Although the mean score value for the right cartilage of the Mg groups (11.25) tend to be higher than these of the WE (8.25) and Drilling (7.625) group, the differences between the groups were not statistically significant (Fig. 7A). In contrast, score values for the left, non-operated cartilage were in a closer range with highest values in the Drilling group (4.625). Again, the difference to the Mg (3.75) and WE (4.0) group were not statistically significant. (Fig. 7A). Exemplary pictures of the Drilling group and Mg group as well as the contralateral, non-operated left side are also shown in Fig. 7B–D.

CD271 stained slices showed different results regarding number of positive cells (CD271+) within the cartilage and number of CD271+ vessels in the subchondral bone.

There were no significant differences between the three groups regarding CD271+ cells in the cartilage of the osteoarthritic knees with a trend for higher number of cells in the Drilling group (median value of 2 (Mg), 1 (WE) and 3 (Drilling)) (Fig. 8). With overall higher values for left, non-operated knees, the difference to the right sides was significant for the Mg (median value 4,  $p = 0.024$ ) and WE (median value 4,  $p = 0.026$ )

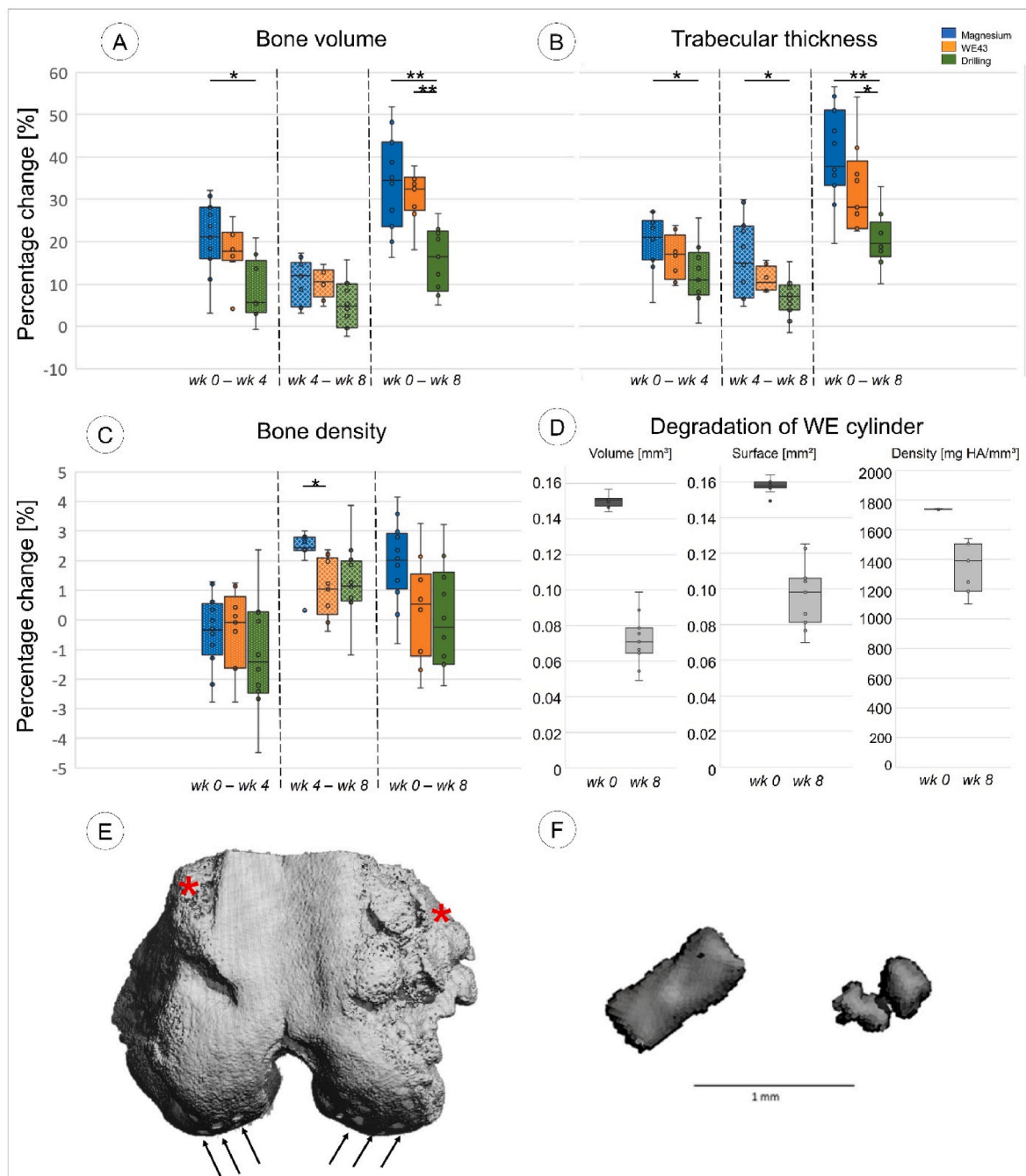


**Fig. 4.** μ-Computed tomographical results of bone changes for the three different scanning intervals (A–C) and volume, surface area and density of WE cylinders (D) at implantation (impl) and euthanization (euth). Blue: Magnesium group, orange: WE43 group, green: Drilling group, Dark grey: WE cylinders at implantation, light grey: WE cylinders at euthanization. \* for significant differences with  $p \leq 0.05$  and \*\* for significant differences with  $p \leq 0.001$ . E: exemplary segmented μCT image of the distal part of the femur after implantation of the cylinders. Black arrows: drill holes; red asterisks: osteophytes. F: exemplary segmented μCT image of WE cylinder at implantation (left) and after eight weeks (right).

group, but not for the Drilling group (median value 4,  $p = 0.1$ ) (Fig. 8). In contrast, the number of CD271+ vessels in the subchondral area of the right, operated femur was significantly higher in the Drilling group ( $51.33 \pm 30.33$ ,  $p = 0.035$ ) compared to the Mg and WE group ( $26.43 \pm 18.77$  and  $27.13 \pm 14.83$ , respectively). The left, non-operated femur showed overall lower levels (Mg:  $21.29 \pm 16.55$ , Drilling:  $29.67 \pm 49.54$ ) except for the WE group ( $39.80 \pm 55.02$ ), and no significant differences between the groups (Fig. 9).

#### 4. Discussion

We evaluated the influence of subchondrally-implanted cylinders of Mg and WE43 on bone, cartilage and pain in an *in vivo* OA rabbit model. Animals, which received only drilling holes, served as control. μCT evaluation showed an obvious impact of Mg and WE43 on bone. The volume and tr. th. of the subchondral bone increased significantly during the eight weeks follow up in both groups with implanted cylinders in comparison to the control group. These results are in accordance with the pilot study, also exhibiting the same timely dynamic with a higher increase in the first scanning interval [26]. Evaluation of

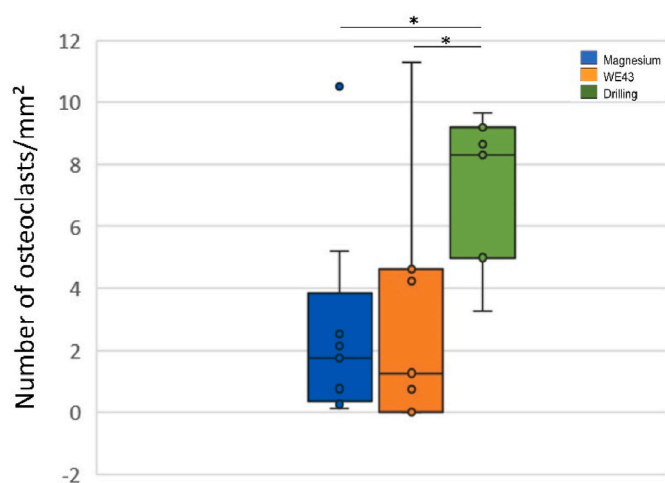


Fig. 5. Number of osteoclasts per mm<sup>2</sup>, calculated in the region of cylinder implantation and drill holes only, respectively. \* indicate significant differences of p ≤ 0.05.

bone-resorbing OC in TRAP-stained tissue slices showed a reduced number of OC after the implantation of Mg and WE43 cylinders compared to the sole drilling holes. A recent study on the influence of intra-articularly injected MgO nanoparticles also showed a reduction of number and area of OC in the Mg groups [32]. They attributed this inhibition of OC formation and function to the suppressed phosphorylation of Akt/protein kinase B [32]. This might also be the case in our study and therewith contributed to the increase in bone volume. The well-known osteoconductive property of Mg and its alloys has been reported manifold proposing different possible mechanisms with Mg ions being in the centre of many of them. According to an equation published by Witte et al. (2008), Mg ionizes to Mg<sup>2+</sup> in an anodic reaction [33]. Therefore, Mg<sup>2+</sup> ions are most likely the reactive part and several studies

support this hypothesis. *In vitro*, Mg chloride increased differentiation of rat bone marrow MSCs and promoted osteogenic differentiation and mineralization [17]. Another study found, that Mg ions induced significantly cell viability, alkaline phosphatase activity and osteocalcin levels of human osteoblasts *in vitro* and promoted the gap junction intercellular communication [23]. In one of the earlier published *in vivo* studies using degradable Mg implants in the bony environment, Witte et al. hypothesized, that the observed increase in mineral apposition rate could be attributed to an enhanced protein translation for the extracellular matrix such as collagen I due to high concentrations of Mg subsequently enhancing osteoid deposition around the Mg implants [30]. Although in our study the overall amount of Mg is rather low due to the small size of the implanted cylinders, the reactive ions formed during degradation of the implants are easily able to develop their pro-osteogenic potential being situated nearby and within the bone marrow. This is also supported by the highly reactive bone marrow region seen in Safranin O-fast green stained slices. The desired bone volume enhancing effect could therefore be achieved by the implantation of Mg and WE43 cylinders. However, an increase in bone volume alone could also be a sign for subchondral sclerosis. Li and Aspden [34] reported already 1997 on bone changes in late stage OA samples without any Mg influence. They evaluated the properties of osteoporotic and osteoarthritic human bone samples and found an increase in subchondral bone volume of around 60 % for OA bone compared to healthy control samples [34]. However, they also showed that the density of the OA bone was decreased by 8.5 % relative to normal bone being equivalent to lower mineralization and mechanical stability. Hunter et al. [35] did a thorough evaluation of bone samples taken from osteoarthritic knees using  $\mu$ CT. They found that samples taken from osteoarthritic knees exhibited increased bone volume fraction and tr. th. while bone mineral density was decreased and concluded that these altered characteristics may influence the mechanical properties of the subchondral trabecular network [35]. The role of biomechanics of the subchondral bone is beyond doubt yet not fully understood. As a highly dynamic structure it adapts to the mechanical forces imposed across the joint [36]. Altered properties such as stiffening or reduction in pliability

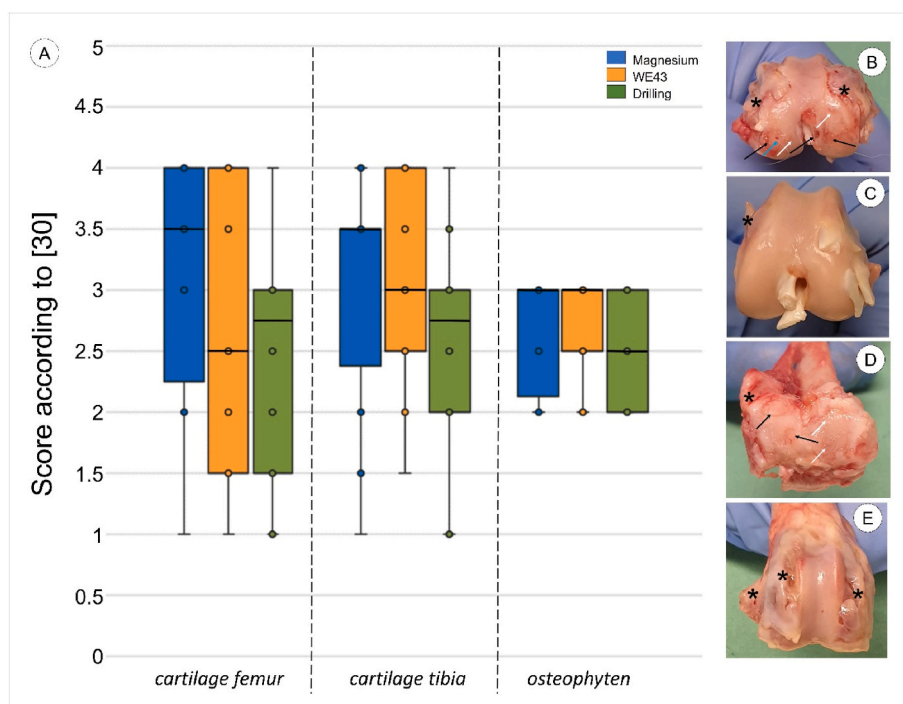
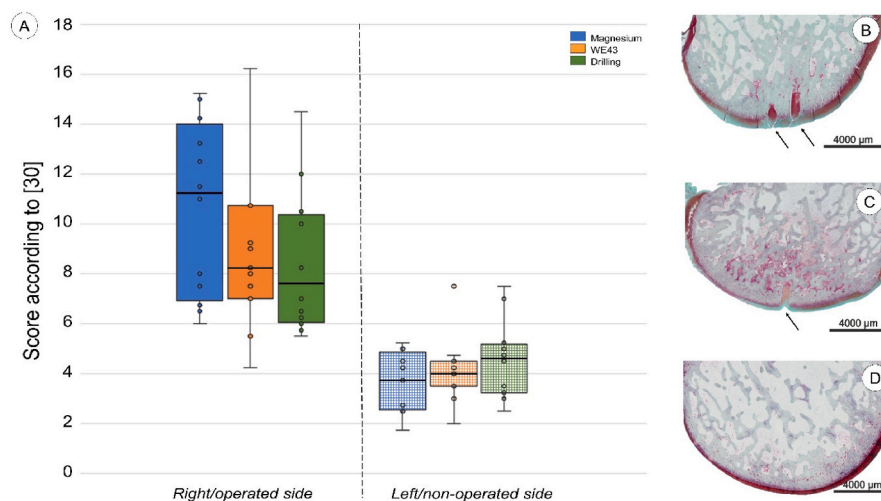
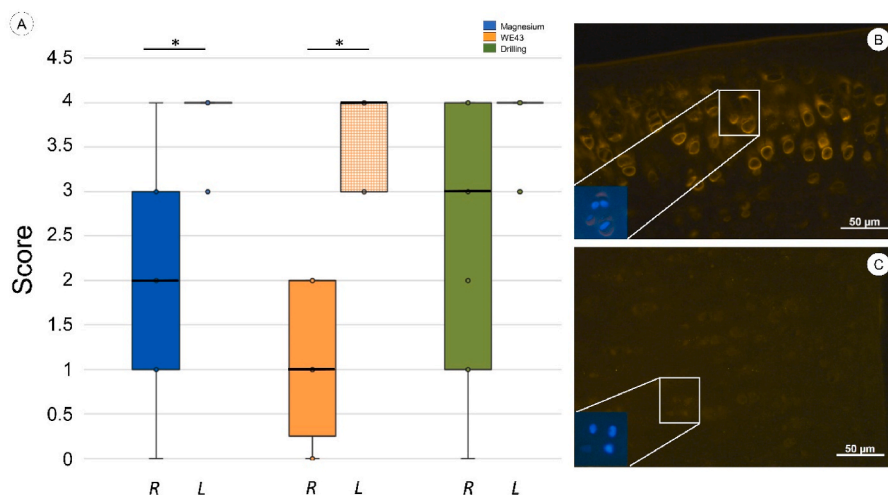


Fig. 6. Results of the macroscopic semi-quantitative scoring (A) according to Ref. [30] and exemplary pictures of higher score values for femoral cartilage, tibial cartilage (D) and osteophytes (E). C shows nearly physiologic condition of left side with only very mild beginning osteophyte formation. Black asterisk: osteophytes; black arrows: deep cartilage lesions; white arrows: softened cartilage; blue arrow: drilling hole.



**Fig. 7.** Results of semi-quantitative scoring according to Ref. [31] for Safranin-O fast green stained slices of right, operated cartilage and left, non-operated cartilage of rabbits eight weeks after treatment of osteoarthritic knees (A). B-D show exemplary pictures of histologic samples of Drilling group (B), Mg group (C) and left, non-operated side (D). Black arrows: drilling holes.



**Fig. 8.** Scoring results of CD271 stained slices of right, operated (R) and left, non-operated (L) cartilage (A) and exemplary histologic pictures for CD271+ cells (B) and CD271-cells (C). Magnification in B and C show triple filter image (using DAPI-FITC-RITC filter) which show the clear positive boundaries of the chondrocytes in B and their absence in C. \* for significant differences with  $p \leq 0.05$ .

could increase the transmission of loads to the overlying cartilage contributing to secondary cartilage degeneration [37] which emphasizes the importance of bone mineral density. Despite the high increase in bone volume in our study, the mineral density after eight weeks of implantation slightly increased in both cylinder groups (1.95 % and 0.57 %) but remained nearly the same in the control group (0.08 %). This might indicate an improved biomechanical characteristic, which could prevent further cartilage degeneration. Yamasaki et al. also found an increase in bone density after implantation of Mg containing specimen [38]. They examined a functionally graded carbonate apatite containing magnesium scaffold, called FGMgCO<sub>3</sub>Ap, in two animal models including rats and rabbits and compared these scaffolds to homogenous apatite containing carbonate without Mg. There was a slight increase in thickness of the crania bone in rats as well as a higher bone formation in femurs of rabbits. Also, the non-magnesium containing scaffold induced bone formation, however bone density was significantly higher in animals that received FGMgCO<sub>3</sub>Ap [38]. They discussed that Mg<sup>2+</sup> ions may be integrated into apatite crystals and therewith accelerate

osteoblast adhesion promoting bone formation [38]. The positive results on subchondral bone volume and bone mineral density in our study leads to the expectation of a likewise positive impact on cartilage condition. But, contrary to the clear influence of the implanted cylinders on bone, there were no significant differences between the groups regarding the condition of the cartilage after eight weeks of implantation. Macroscopically, all groups showed scores around 3 with no differences between femur and tibia. In the Mg group, changes appeared to be significantly more severe than in the pilot study, were median values for femur and tibia were 1 and 2.5, respectively [26]. While minimum values of 1 occurred in Mg and Drilling group in this study, lowest score in the pilot study was 0 equivalent to the presence of single animals with intact cartilage. However, since the maximum value for both studies was four, the difference in median values could be attributed either to the higher number of individuals or just coincidence. Results of Safranin O/fast green stained slices were in conformity with the macroscopic findings. There were neither significant differences between the groups regarding right, operated knees nor left, non-operated ones. OARSi score

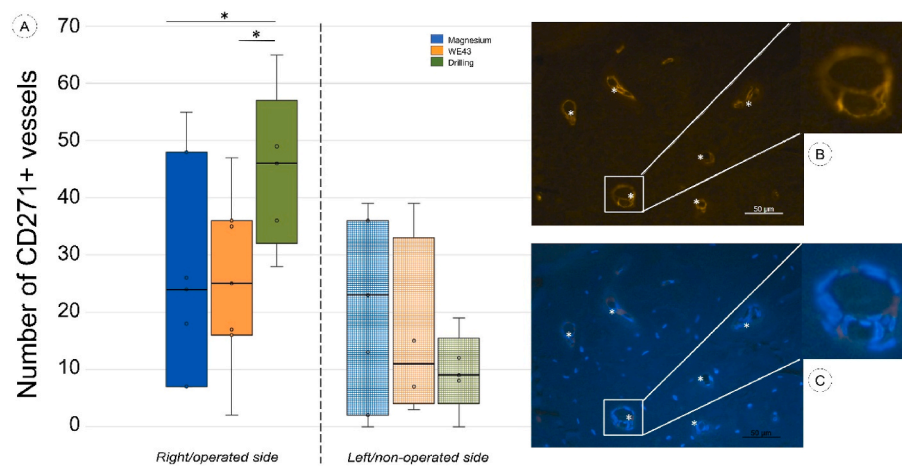


**Fig. 9.** Counting results of CD271+ vessels in right, operated and left, non-operated histological samples (A) and exemplary histologic pictures for CD271+ vessels in a sample of the drilling group (B, C). B shows RITC-filter image with magnification of one of the CD271+ vessels. C shows the same field of view as triple filter image (using DAPI-FITC-RITC filter). White asterisk: CD271+ vessels. \* for significant differences with  $p \leq 0.05$ .

is well established and recommended to evaluate cartilage changes in different species like mice [39], rats [40], guinea pigs [41], rabbits [31], as well as sheep and goats [42]. Paglia et al. evaluated the influence of two orally administered drugs on cartilage in a rat model of OA [43]. They found significantly elevated OARSI scores for the treated, medial parts of the tibia seven weeks after OA induction by destabilization of the medial meniscus (DMM) [43]. Notably, they also found distinctly higher scores in the sham operated knees where no DMM was performed five weeks after surgery. While they did not discuss the differences between DMM and sham operated groups, influence of increased loading of the non-affected limb due to pain-related unloading of the OA limb is known and subject of different studies [44–46]. Radiographic [45] and histological [44] features of early OA were present in contralateral sides of OA joints. Zhou et al. specifically examined the influence of joint immobilization for OA induction on the contralateral mobile joint in rabbits [46]. They showed OARSI scores of around 10 in the contralateral joint eight weeks after immobilization of the other limb and mention abnormal mechanical loads and peri-articular soft tissue changes as decrease in muscle mass or muscle hypertrophy as possible reasons [46].

In our study, also increased values of the non-operated, left knees were found eight weeks after second surgery indicating onset of OA with no differences between the groups. Also, CD271 staining showed no positive influence of Mg or WE43 implantation on cartilage compared to sole drilling. CD271, which in the literature is also referred to as p75, is present in sensory and sympathetic nerve fibres, that are most often situated close to blood vessels, as well as in cells within the articular cartilage [47,48]. It is a low-affinity neurotrophin receptor [49]. Neurotrophins are known to have essential effects for the nervous system [50] and chondrocytes [51]. Grimsholm et al. found significantly decreased numbers of p75+ cells in the cartilage of severely arthritic mice [49]. In combination with an often observed reduction in the total amount of lining cartilage they concluded that arthritis leads to decreased effects of neurotrophins at the level of cartilage lining the joint cavity [49]. We also found by trend reduced numbers of p75+/CD271+ cells in the articular cartilage of rabbits after implantation of Mg and WE43 compared to sole drilling indicating the clear osteoarthritic condition.

During the pilot study, contralateral knees of Mg treated rabbits showed better condition of articular cartilage than in the control group [26]. That led to the hypothesis that Mg implants might have resulted in less pain compared to sole drilling which could not be detected by scoring of lameness. Therefore, we led special focus on the evaluation of certain pain indicators. Although CD271 staining could not show a

positive influence of Mg and WE43 on the regenerative capacity of the cartilage, it could unveil an impact on CD271+ vessels. As mentioned above, CD271 is present in sensory and sympathetic nerve fibres around vessels [47]. Pain in OA is the main symptom and predominant factor for its crucial economic role and numerous structures are involved as for example synovitis, subchondral bone marrow lesions, sprouting of nerve fibres and osteophyte formation [7,9,47]. Pain mechanisms are not yet clarified which impedes the development of successful treatment options and recent reviews on OA emphasize the importance of understanding pain [52,53]. According to a review by O'Neill and Felson, bone marrow lesions (BML) and inflammatory cytokines may play an important role [54]. Noxious stimuli that trigger OA nociceptors could be physical/mechanical or chemical. Overall, inflammation/synovitis is often referred to as a major cause of pain in OA [55–57]. While Perry et al. found no association between BML volume and knee pain, they showed that synovial tissue volume as sign for synovitis/inflammatory condition of the knee and pain was positively correlated [58]. Inflamed synovial tissue secretes a number of cytokines including mediators like tumor necrosis factor (TNF)- $\alpha$ , interleukin (IL)-1 $\beta$ , IL-6, or bradykinin, prostaglandin E2 [54,57] which could initiate action potentials at the terminal endings of peripheral nerves [59]. Transmission of these potentials by unmyelinated C nerve fibres leads to the burning pain which is typically described by OA patients. Such nerve fibers, which accompany new sprouted vessels in OA, are suggested to be a source of pain in OA [9]. Also, Del Rey showed that perivascular CD271+ stromal cells were extended in OA and RA (rheumatoid arthritis) and exhibited elevated pro-inflammatory properties [60]. While Mizuno et al. classified the specific role of CD271+ in the perivascular region as unknown, they also emphasize their possible role in the pathophysiological response of vessels and neurogenesis during active synovitis of OA [61]. The lower number of CD271+ vessels in Mg and WE43 implanted animals in our investigation might indicate a reduced pain perception and gives reason to expect a lower grade or shorter lasting lameness of rabbits after implantation of Mg and WE43. Also, Mapp et al. showed a clear correlation of the number of vessels and pain in an *in vivo* rat model of OA [62]. After initiation of OA by medial meniscal transection and treatment with different doses of metallo matrixproteinase inhibitor they evaluated the number of vessels at the osteochondral junction in toluidine blue stained slices and weight-bearing asymmetry by incapacitation up to 35 days after surgery. They found significant reduced pain in animals with significant lower quantities of vessels. However, they did not perform a specific staining regarding neural structures within the vessel walls [62]. In our study, the expected impact of reduced CD271+ vessels could neither be seen in the pain score nor in the gait analysis.

According to the mean score values, animals showed obvious, moderate lameness one week after implantation which already improved until the next week. Normal motion in all animals was shown in week five after implantation. None of these results differed between the groups, which was comparable to the pilot study [26]. As intended, implementation of the higher sensitive sensor mat enabled closer consideration of the course of lameness. However, also this more sensitive evaluation could not show any differences between the groups. As seen in the active pain score, all animals showed a distinct unloading of the operated hind limb one week after implantation. Differently to the score, it seemed that animals of the WE43 recovered slightly faster than the others, although on no statistically significant level. After eight weeks, a shift of load bearing to the non-operated side could still be detected in all groups. In contrast to our results, Yao et al. could show a decreasing effect of Mg ions in combination with vitamin C application on pain expressed by enhanced gait pattern as shown in catwalk analyses [25]. However, most distinct effects could be seen in the earlier time points. Furthermore, it has to be kept in mind that they started their treatment at week 2 post surgery and classified their model as early stage which might contribute to the positive results. The effect of enhanced gait pattern was consistent with their results regarding inhibition of osteophyte formation and production of pain related neuropeptides. In our study, all animals exhibited distinct osteophyte formation with no significant differences between the groups. Therefore, it may be possible that osteophyte related pain stimuli may obscure the positive effect of reduced CD271+ vessels quantity. More specific evaluation should consider these thoughts in future studies. An additional positive result of Yao et al. was the promotion of M2 polarization of synovial macrophages [25], which additionally places emphasis on the impact of inflammatory condition. A very recent study by members of the same group, already referenced above, also showed a positive influence of Mg<sup>2+</sup> on pain in an *in vivo* OA rat model [32]. They administered the MgO-nanoparticles during the surgery of OA onset by transection of the lateral ligament and meniscectomy. Therefore, their approach has to be classified as protective rather than treating clinically manifest OA. However, they showed a distinct protective influence of the nanoparticles with significantly increased pain threshold in Von Frey pain test and decreased spatial symmetry using calculations of step length and stride length [32]. They also showed a clear chondroprotective influence *in vitro* with enhanced chondrogenic differentiation and inhibition of chondrocyte apoptosis [32]. Although they did not perform gait analysis or similar pain related evaluation, also Yao et al. showed a clear anti-osteoarthritic effect *in vivo* [55]. They used MgCl<sub>2</sub> injections to treat experimental PTOA in rats and found alleviation of cartilage degeneration and synovitis.

Why the positive results of implanted Mg and WE43 cylinders on subchondral bone and CD271+ vessels did lead to neither enhanced quality of articular cartilage nor pain sensation in our study in rabbits could not be clearly answered yet. Possibly, the amount of Mg<sup>2+</sup> ions available for impacting cartilage as in Ref. [25] was not high enough triggering only bony reactions. Alternatively, the distance from inside the subchondral bone to the joint was too far as the positive influence of Mg<sup>2+</sup> ions in mice by Yao et al. was induced after intraarticular injection and therewith in direct contact to the chondrocytes. Furthermore, rabbits in our study exhibited distinct osteophyte formation, which – as known as one major pain inductor – may obscure possible effects on pain. Another factor, which might influence pain sensation is the extracapsular fixation of the joint instability during the second surgery. While there are no pain related studies in rabbits after application of this technique dogs have been evaluated as species with high prevalence of anterior cruciate ligament ruptures. Au et al. examined two different treatment options for cranial ligament disease in dogs [63]. They used a pressure plate to measure peak vertical forces (PVF) in gait analysis and showed continued increase in PVF in the two years follow-up. While values were significantly below the preoperative/pathological levels three weeks after surgery, they clearly exceeded these values five weeks

post-surgery indicating the effectiveness of the treatment [63]. However, also OA scores evaluated by radiographs increased during the two years follow-up. This might be indicative of an insufficient restoration of the healthy biomechanical situation of the knee joint. On the other hand, Del Carpio et al. performed three-dimensional kinematic examinations of knee joints fixed by lateral suture stabilization *in vitro*. They showed that the physiological 3D-kinematics were successfully restored using LLS and suggested that biomechanical insufficiency is not mainly causative for suboptimal clinical outcomes [64]. Independent of the fact that the fixation technique used in our study might have an influence on pain or OA progression, this impact is present in all groups equally and should therefore not compromise the assessment of group-dependant differences. Lastly, different evaluation periods should be considered, not only for establishment of OA (early – mid – late stage OA) but also for follow-up period which might involve later evaluation points.

## 5. Conclusions

*In vivo* implantation of Mg and WE43 cylinder into the subchondral bone of osteoarthritic rabbits for eight weeks led to more than 30 % increase in bone volume and trabecular thickness while bone mineral density also slightly increased. As representative for pain, a higher number of CD271+ vessels were present in control samples without magnesium. These results indicate favored biomechanical properties of the trabecular network beneath the joint cartilage and gave reason to expect a positive effect on pain sensation. However, no impact could be found on the further progression of cartilage degeneration and grade of lameness. Therewith, although relevant structures for OA progression and pain sensation could be positively influenced by implanted cylinders of Mg and WE43, this treatment failed to achieve clinical relevance, especially regarding pain. Possible reasons might be an insufficient amount of magnesium to impact not only bone but also cartilage, an excessive distance between implanted cylinders and cartilage or an insufficient time interval to allow the positive changes in structure to affect also the cartilage. Furthermore, rabbits in our study exhibited distinct osteophyte formation, which – as known as one major pain inductor – may obscure possible effects on pain. Therefore, subsequent studies should further deepen evaluation methods regarding pain mechanisms including amongst others the synovial membrane, osteophytes and bone marrow lesions as well as lay focus on additional possibilities to deliver magnesium in adequate quantity to all relevant locations and consider prolonged follow-up periods. Changes in pain relevant structures should be monitored more thoroughly including thickness and cell composition of synovial tissue samples, evaluation of inflammatory markers and differentiation of nerve structures and pain mediators using more specific markers.

## Ethics approval and consent to participate

The animal experiments were performed according to the German Animal Welfare act and EU Directive 2010/63/EU after approval by the responsible authority “Lower Saxony State Office for Consumer Protection and Food Safety” (LAVES) under registration number 33.9-42502-04-18/2774.

Respective information are also included in the manuscript.

## CRediT authorship contribution statement

**Nina Angrisani:** Writing – original draft, Visualization, Validation, Supervision, Project administration, Methodology, Investigation, Funding acquisition, Formal analysis, Data curation. **Christin von der Ahe:** Writing – review & editing, Methodology, Investigation, Formal analysis. **Regine Willumeit-Römer:** Writing – review & editing, Resources, Project administration, Funding acquisition. **Henning Windhagen:** Writing – review & editing, Supervision, Resources, Conceptualization. **Verena Scheper:** Writing – review & editing,

Validation, Resources. **Michael Schwarze:** Writing – review & editing, Methodology, Formal analysis, Data curation. **Björn Wiese:** Writing – review & editing, Investigation, Formal analysis, Data curation. **Heike Helmholz:** Writing – review & editing, Investigation, Formal analysis, Data curation. **Janin Reifenrath:** Writing – review & editing, Validation, Supervision, Project administration, Methodology, Investigation, Formal analysis, Data curation, Conceptualization.

### Declaration of Competing interest

All authors declare that they have no conflicts of interest.

### Acknowledgements

The authors thank Heidi Harting, Merle Kempfert, Hannah Marahrens, Diana Strauch and Parmida Khazalian for excellent technical assistance and Holger Neumann from novel GmbH for trouble shooting with software problems.

This work was funded by the German Research Foundation (Deutsche Forschungsgesellschaft, DFG, grant numbers 404534760).

### Appendix A. Supplementary data

Supplementary data to this article can be found online at <https://doi.org/10.1016/j.bioactmat.2024.06.003>.

### References

- [1] GBD 2021 Osteoarthritis Collaborators. Global, regional, and national burden of osteoarthritis, 1990–2020 and projections to 2050: a systematic analysis for the Global Burden of Disease Study 2021. *Lancet Rheumatol* 5 (9) (2023 August 21) e508–e522, [https://doi.org/10.1016/S2665-9913\(23\)00163-7](https://doi.org/10.1016/S2665-9913(23)00163-7).
- [2] D.J. Hunter, S. Bierma-Zeinstra, *Osteoarthritis*, *Lancet* 393 (10182) (2019 April 27) 1745–1759, [https://doi.org/10.1016/S0140-6736\(19\)30417-9](https://doi.org/10.1016/S0140-6736(19)30417-9).
- [3] V.P. Leifer, J.N. Katz, E. Losina, The burden of OA-health services and economics, *Osteoarthritis Cartilage* 30 (1) (2022 January 01) 10–16, <https://doi.org/10.1016/j.joca.2021.05.007>.
- [4] K.D. Brandt, E.L. Radin, P.A. Dieppe, L. van de Putte, Yet more evidence that osteoarthritis is not a cartilage disease, *Ann. Rheum. Dis.* 65 (10) (2006 October 01) 1261–1264, <https://doi.org/10.1136/ard.2006.058347>.
- [5] H. Long, Q. Liu, H. Yin, K. Wang, N. Diao, Y. Zhang, et al., Prevalence trends of site-specific osteoarthritis from 1990 to 2019: findings from the global burden of disease study 2019, *Arthritis Rheumatol*. 74 (7) (2022 July 01) 1172–1183, <https://doi.org/10.1002/art.42089>.
- [6] M.T. Hannan, D.T. Felson, T. Pincus, Analysis of the discordance between radiographic changes and knee pain in osteoarthritis of the knee, *J. Rheumatol.* 27 (6) (2000 June 01) 1513–1517.
- [7] D.J. Hunter, A. Guermazi, F. Roemer, Y. Zhang, T. Neogi, Structural correlates of pain in joints with osteoarthritis, *Osteoarthritis Cartilage* 21 (9) (2013 September 01) 1170–1178, <https://doi.org/10.1016/j.joca.2013.05.017>.
- [8] T.W. O'Neill, D.T. Felson, Mechanisms of osteoarthritis (OA) pain, *Curr. Osteoporos. Rep.* 16 (5) (2018 October 01) 611–616, <https://doi.org/10.1007/s11914-018-0477-1>.
- [9] S. Suri, S.E. Gill, S. Massena de Camin, D. Wilson, D.F. McWilliams, D.A. Walsh, Neurovascular invasion at the osteochondral junction and in osteophytes in osteoarthritis, *Ann. Rheum. Dis.* 66 (11) (2007 November 01) 1423–1428, <https://doi.org/10.1136/ard.2006.063354>.
- [10] E. Willbold, A. Weizbauer, A. Loos, J.M. Seitz, N. Angrisani, H. Windhagen, et al., Magnesium alloys: a stony pathway from intensive research to clinical reality. Different test methods and approval-related considerations, *J. Biomed. Mater. Res.* 105 (1) (2017 January 01) 329–347, <https://doi.org/10.1002/jbm.a.35893>.
- [11] H. Yang, B. Jia, Z. Zhang, X. Qu, G. Li, W. Lin, et al., Alloying design of biodegradable zinc as promising bone implants for load-bearing applications, *Nat. Commun.* 11 (1) (2020 January 21) 401–407, <https://doi.org/10.1038/s41467-019-14153-7>.
- [12] A.H. Martinez Sanchez, B.J.C. Luthringer, F. Feyerabend, R. Willumeit, Mg and Mg alloys: how comparable are in vitro and in vivo corrosion rates? A review, *Acta Biomater.* 13 (2015 February 01) 16–31, <https://doi.org/10.1016/j.actbio.2014.11.048>.
- [13] J. Chen, L. Tan, X. Yu, I.P. Etim, M. Ibrahim, K. Yang, Mechanical properties of magnesium alloys for medical application: a review, *J. Mech. Behav. Biomed. Mater.* 87 (2018 November 01) 68–79, <https://doi.org/10.1016/j.jmbm.2018.07.022>.
- [14] Z.P. Kacarevic, P. Rider, A. Elad, D. Tadic, D. Rothamel, G. Sauer, et al., Biodegradable magnesium fixation screw for barrier membranes used in guided bone regeneration, *Bioact. Mater.* 14 (2021 December 02) 15–30, <https://doi.org/10.1016/j.bioactmat.2021.10.036>.
- [15] A. Turan, Y.A. Kati, B. Acar, O. Kose, Magnesium bioabsorbable screw fixation of radial styloid fractures: case report, *J. Wrist Surg.* 9 (2) (2020 April 01) 150–155, <https://doi.org/10.1055/s-0039-1685489>.
- [16] A. Sahin, D. Gulabi, H. Buyukdogan, A. Agar, B. Kilic, I. Mutlu, et al., Is the magnesium screw as stable as the titanium screw in the fixation of first metatarsal distal chevron osteotomy? A comparative biomechanical study on sawbones models, *J. Orthop. Surg.* 29 (3) (2021 December 01) 23094990211056439, <https://doi.org/10.1177/23094990211056439>.
- [17] J.M. Diaz-Tocados, C. Herencia, J.M. Martinez-Moreno, A. Montes de Oca, M. E. Rodriguez-Ortiz, N. Vergara, et al., Magnesium chloride promotes osteogenesis through notch signaling activation and expansion of mesenchymal stem cells, *Sci. Rep.* 7 (1) (2017 August 10) 7839–y, <https://doi.org/10.1038/s41598-017-08379-y>.
- [18] F. Witte, V. Kaese, H. Haferkamp, E. Switzer, A. Meyer-Lindenberg, C.J. Wirth, et al., In vivo corrosion of four magnesium alloys and the associated bone response, *Biomaterials* 26 (17) (2005 June 01) 3557–3563, [https://doi.org/10.1016/S0142-9612\(04\)00876-2](https://doi.org/10.1016/S0142-9612(04)00876-2) [pii].
- [19] M.N. Sarian, N. Iqbal, P. Sotoudehbagha, M. Razavi, Q.U. Ahmed, C. Sukotjo, et al., Potential bioactive coating system for high-performance absorbable magnesium bone implants, *Bioact. Mater.* 12 (2021 October 27) 42–63, <https://doi.org/10.1016/j.bioactmat.2021.10.034>.
- [20] Li Ye, J. Xu, J. Mi, X. He, Q. Pan, L. Zheng, et al., Biodegradable magnesium combined with distraction osteogenesis synergistically stimulates bone tissue regeneration via CGRP-FAK-VEGF signaling axis, *Biomaterials* 275 (2021 August 01) 120984, <https://doi.org/10.1016/j.biomaterials.2021.120984>.
- [21] A. Bernhardt, H. Helmholz, D. Kilian, R. Willumeit-Romer, M. Gelinsky, Impact of degradable magnesium implants on osteocytes in single and triple cultures, *Biomater. Adv.* 134 (2022 March 01) 112692, <https://doi.org/10.1016/j.msec.2022.112692>.
- [22] X. Kuang, J. Chiou, K. Lo, C. Wen, Magnesium in joint health and osteoarthritis, *Nutr. Res.* 90 (2021 June 01) 24–35, <https://doi.org/10.1016/j.nutres.2021.03.002>.
- [23] L.Y. He, X.M. Zhang, B. Liu, Y. Tian, W.H. Ma, Effect of magnesium ion on human osteoblast activity, *Braz. J. Med. Biol. Res.* 49 (7) (2016 July 04) e2527, <https://doi.org/10.1590/1414-431X20165257>, [10.1590/1414-431X20165257](https://doi.org/10.1590/1414-431X20165257).
- [24] F. Feyerabend, F. Witte, M. Kammal, R. Willumeit, Unphysiologically high magnesium concentrations support chondrocyte proliferation and redifferentiation, *Tissue Eng.* 12 (12) (2006 December 01) 3545–3556, <https://doi.org/10.1089/ten.2006.12.3545>.
- [25] H. Yao, J. Xu, J. Wang, Y. Zhang, N. Zheng, J. Yue, et al., Combination of magnesium ions and vitamin C alleviates synovitis and osteophyte formation in osteoarthritis of mice, *Bioact. Mater.* 6 (5) (2020 November 10) 1341–1352, <https://doi.org/10.1016/j.bioactmat.2020.10.016>.
- [26] N. Angrisani, R. Willumeit-Romer, H. Windhagen, B. Mavila Chathoth, V. Schepel, B. Wiese, et al., Small-sized magnesium cylinders influence subchondral bone quality in osteoarthritic rabbits - an in vivo pilot study, *Eur. Cell. Mater.* 42 (2021 September 28) 179–195, <https://doi.org/10.22023/eCM.v042a14>.
- [27] M.A. van Zuijlen, P.W.F. Vrolijk, M.A.G. van der Heyden, Bilateral successive cranial cruciate ligament rupture treated by extracapsular stabilization surgery in a pet rabbit (*Oryctolagus cuniculus*), *J. Exot. Pet Med.* 19 (3) (2010) 245–248, <https://doi.org/10.1053/j.jepm.2010.07.009>.
- [28] C. von der Ahe, H. Marahrens, M. Schwarze, N. Angrisani, J. Reifenrath, Pressure sensing mat as an objective and sensitive tool for the evaluation of lameness in rabbits, *PLoS One* 18 (7) (2023 July 07) e0286918, <https://doi.org/10.1371/journal.pone.0286918>.
- [29] R.O. Robinson, W. Herzog, B.M. Nigg, Use of force platform variables to quantify the effects of chiropractic manipulation on gait symmetry, *J. Manip. Physiol. Ther.* 10 (4) (1987 August 01) 172–176.
- [30] F. Witte, J. Fischer, J. Nellesen, C. Vogt, J. Vogt, T. Donath, et al., In vivo corrosion and corrosion protection of magnesium alloy LAE442, *Acta Biomater.* 6 (5) (2010 May 01) 1792–1799, <https://doi.org/10.1016/j.actbio.2009.10.012>.
- [31] S. Lavery, C.A. Girard, J.M. Williams, E.B. Hunziker, K.P. Pritzker, The OARSI histopathology initiative - recommendations for histological assessments of osteoarthritis in the rabbit, *Osteoarthritis Cartilage* 18 (Suppl 3) (2010 October 01) 53, <https://doi.org/10.1016/j.joca.2010.05.029>.
- [32] L. Zheng, S. Zhao, Y. Li, J. Xu, W. Yan, B. Guo, et al., Engineered MgO nanoparticles for cartilage-bone synergistic therapy, *Sci. Adv.* 10 (10) (2024 March 08) eadk6084, <https://doi.org/10.1126/sciadv.adk6084>.
- [33] P. Bajger, J.M.A. Ashbourn, V. Manhas, Y. Guyot, K. Lietaert, L. Geris, Mathematical modelling of the degradation behaviour of biodegradable metals, *Biomech. Model. Mechanobiol.* 16 (1) (2017 February 01) 227–238, <https://doi.org/10.1007/s10237-016-0812-3>.
- [34] B. Li, R.M. Aspden, Composition and mechanical properties of cancellous bone from the femoral head of patients with osteoporosis or osteoarthritis, *J. Bone Miner. Res.* 12 (4) (1997 Apr) 641–651, <https://doi.org/10.1359/jbmr.1997.12.4.641>.
- [35] D.J. Hunter, L. Gerstenfeld, G. Bishop, A.D. Davis, Z.D. Mason, T.A. Einhorn, et al., Bone marrow lesions from osteoarthritis knees are characterized by sclerotic bone that is less well mineralized, *Arthritis Res. Ther.* 11 (1) (2009) R11, <https://doi.org/10.1186/ar2601>.
- [36] G. Li, J. Yin, J. Gao, T.S. Cheng, N.J. Pavlos, C. Zhang, et al., Subchondral bone in osteoarthritis: insight into risk factors and microstructural changes, *Arthritis Res. Ther.* 15 (6) (2013) 223, <https://doi.org/10.1186/ar4405>.
- [37] M.B. Goldring, S.R. Goldring, Articular cartilage and subchondral bone in the pathogenesis of osteoarthritis, *Ann. N. Y. Acad. Sci.* 1192 (2010 March 01) 230–237, <https://doi.org/10.1111/j.1749-6632.2009.05240.x>.

- [38] Y. Yamasaki, Y. Yoshida, M. Okazaki, A. Shimazu, T. Kubo, Y. Akagawa, et al., Action of FGMgCO3Ap-collagen composite in promoting bone formation, *Biomaterials* 24 (27) (2003 December 01) 4913–4920, [https://doi.org/10.1016/S0142-9612\(03\)00414-9](https://doi.org/10.1016/S0142-9612(03)00414-9).
- [39] S.S. Glasson, M.G. Chambers, W.B. Van Den Berg, C.B. Little, The OARSI histopathology initiative - recommendations for histological assessments of osteoarthritis in the mouse, *Osteoarthritis Cartilage* 18 (Suppl 3) (2010 October 01) 17, <https://doi.org/10.1016/j.joca.2010.05.025>.
- [40] N. Gerwin, A.M. Bendele, S. Glasson, C.S. Carlson, The OARSI histopathology initiative - recommendations for histological assessments of osteoarthritis in the rat, *Osteoarthritis Cartilage* 18 (Suppl 3) (2010 October 01) 24, <https://doi.org/10.1016/j.joca.2010.05.030>.
- [41] V.B. Kraus, J.L. Huebner, J. DeGroot, A. Bendele, The OARSI histopathology initiative - recommendations for histological assessments of osteoarthritis in the Guinea pig, *Osteoarthritis Cartilage* 18 (Suppl 3) (2010 October 01) 35, <https://doi.org/10.1016/j.joca.2010.04.015>. Suppl 3.
- [42] C.B. Little, M.M. Smith, M.A. Cake, R.A. Read, M.J. Murphy, F.P. Barry, The OARSI histopathology initiative - recommendations for histological assessments of osteoarthritis in sheep and goats, *Osteoarthritis Cartilage* 18 (Suppl 3) (2010 October 01) 80, <https://doi.org/10.1016/j.joca.2010.04.016>.
- [43] D.N. Paglia, D. Kanjilal, Y. Kadkoy, S. Moskonas, C. Wetterstrand, A. Lin, et al., Naproxen treatment inhibits articular cartilage loss in a rat model of osteoarthritis, *J. Orthop. Res.* 39 (10) (2021 October 01) 2252–2259, <https://doi.org/10.1002/jor.24937>.
- [44] W.A. Cohen, J.M. Servais, I. Polur, Y. Li, L. Xu, Articular cartilage degeneration in the contralateral non-surgical temporomandibular joint in mice with a unilateral partial discectomy, *J. Oral Pathol. Med.* 43 (2) (2014 February 01) 162–165, <https://doi.org/10.1111/jop.12113>.
- [45] F. Eckstein, S. Maschek, F.W. Roemer, G.N. Duda, L. Sharma, W. Wirth, Cartilage loss in radiographically normal knees depends on radiographic status of the contralateral knee - data from the Osteoarthritis Initiative, *Osteoarthritis Cartilage* 27 (2) (2019 February 01) 273–277, <https://doi.org/10.1016/j.joca.2018.10.006>.
- [46] Q. Zhou, B. Wei, S. Liu, F. Mao, X. Zhang, J. Hu, et al., Cartilage matrix changes in contralateral mobile knees in a rabbit model of osteoarthritis induced by immobilization, *BMC Musculoskelet Disord* 16 (2015 August 25) 224–y, <https://doi.org/10.1186/s12891-015-0679-y>.
- [47] S.R. Chartier, S.A. Mitchell, L.A. Majuta, P.W. Mantyh, Immunohistochemical localization of nerve growth factor, tropomyosin receptor kinase A, and p75 in the bone and articular cartilage of the mouse femur, *Mol. Pain* 13 (2017 December 01) 1744806917745465, <https://doi.org/10.1177/1744806917745465>.
- [48] A. Gigante, C. Bevilacqua, A. Pagnotta, S. Manzotti, A. Toesca, F. Greco, Expression of NGF, Trka and p75 in human cartilage, *Eur. J. Histochem.* 47 (4) (2003) 339–344.
- [49] O. Grimsholm, Y. Guo, T. Ny, S. Forsgren, Expression patterns of neurotrophins and neurotrophin receptors in articular chondrocytes and inflammatory infiltrates in knee joint arthritis, *Cells Tissues Organs* 188 (3) (2008) 299–309, <https://doi.org/10.1159/000121432>.
- [50] S. Linnarsson, C.A. Willson, P. Ernfors, Cell death in regenerating populations of neurons in BDNF mutant mice, *Brain Res Mol Brain Res* 75 (1) (2000 January 10) 61–69, [https://doi.org/10.1016/S0169-328X\(99\)00295-8](https://doi.org/10.1016/S0169-328X(99)00295-8).
- [51] F. Iannone, C. De Bari, F. Dell'Accio, M. Covelli, V. Patella, Bianco G. Lo, et al., Increased expression of nerve growth factor (NGF) and high affinity NGF receptor (p140 Trka) in human osteoarthritic chondrocytes, *Rheumatology* 41 (12) (2002 December 01) 1413–1418, <https://doi.org/10.1093/rheumatology/41.12.1413>.
- [52] M. Alves-Simoes, Rodent models of knee osteoarthritis for pain research, *Osteoarthritis Cartilage* 30 (6) (2022 June 01) 802–814, <https://doi.org/10.1016/j.joca.2022.01.010>.
- [53] T.L. Vincent, Peripheral pain mechanisms in osteoarthritis, *Pain* 161 (Suppl 1) (2020 September 01) S138–S146, <https://doi.org/10.1097/j.pain.0000000000001923>, 1.
- [54] T.W. O'Neill, D.T. Felson, Mechanisms of osteoarthritis (OA) pain, *Curr. Osteoporos. Rep.* 16 (5) (2018 October 01) 611–616, <https://doi.org/10.1007/s11914-018-0477-1>.
- [55] H. Yao, J.K. Xu, N.Y. Zheng, J.L. Wang, S.W. Mok, Y.W. Lee, et al., Intra-articular injection of magnesium chloride attenuates osteoarthritis progression in rats, *Osteoarthritis Cartilage* 27 (12) (2019 December 01) 1811–1821, <https://doi.org/10.1016/j.joca.2019.08.007>.
- [56] D. Loeuille, I. Chary-Valckenaere, J. Champigneulle, A. Rat, F. Toussaint, A. Pinzano-Watrin, et al., Macroscopic and microscopic features of synovial membrane inflammation in the osteoarthritic knee: correlating magnetic resonance imaging findings with disease severity, *Arthritis Rheum.* 52 (11) (2005 November 01) 3492–3501, <https://doi.org/10.1002/art.21373>.
- [57] C.R. Scanzello, Chemokines and inflammation in osteoarthritis: insights from patients and animal models, *J. Orthop. Res.* 35 (4) (2017 April 01) 735–739, <https://doi.org/10.1002/jor.23471>.
- [58] T.A. Perry, M.J. Parkes, R.J. Hodgson, D.T. Felson, N.K. Arden, T.W. O'Neill, Association between Bone marrow lesions & synovitis and symptoms in symptomatic knee osteoarthritis, *Osteoarthritis Cartilage* 28 (3) (2020 March 01) 316–323, <https://doi.org/10.1016/j.joca.2019.12.002>.
- [59] H. Schaible, Nociceptive neurons detect cytokines in arthritis, *Arthritis Res. Ther.* 16 (5) (2014) 470–478, <https://doi.org/10.1186/s13075-014-0470-8>.
- [60] M.J. Del Rey, R. Fare, A. Usategui, J.D. Canete, B. Bravo, M. Galindo, et al., CD271(+) stromal cells expand in arthritic synovium and exhibit a proinflammatory phenotype, *Arthritis Res. Ther.* 18 (2016 March 15) 66, <https://doi.org/10.1186/s13075-016-0966-5>, 5.
- [61] M. Mizuno, H. Katano, Y. Mabuchi, Y. Ogata, S. Ichinose, S. Fujii, et al., Specific markers and properties of synovial mesenchymal stem cells in the surface, stromal, and perivascular regions, *Stem Cell Res.* 9 (1) (2018 May 02) 123–129, <https://doi.org/10.1186/s13287-018-0870-9>.
- [62] P.I. Mapp, D.A. Walsh, J. Bowyer, R.A. Maciewicz, Effects of a metalloproteinase inhibitor on osteochondral angiogenesis, chondropathy and pain behavior in a rat model of osteoarthritis, *Osteoarthritis Cartilage* 18 (4) (2010 April 01) 593–600, <https://doi.org/10.1016/j.joca.2009.12.006>.
- [63] K.K. Au, W.J. Gordon-Evans, D. Dunning, K.J. O'Dell-Anderson, K.E. Knap, D. Griffon, et al., Comparison of short- and long-term function and radiographic osteoarthrosis in dogs after postoperative physical rehabilitation and tibial plateau leveling osteotomy or lateral fabellar suture stabilization, *Vet. Surg.* 39 (2) (2010 February 01) 173–180, <https://doi.org/10.1111/j.1532-950X.2009.00628.x>.
- [64] L. Del Carpio, Y. Petit, L. Diotalevi, E. Laroche, A. Levasseur, B. Lussier, Three-dimensional kinematic evaluation of lateral suture stabilization in an in vitro canine cranial cruciate deficient stifle model, *PLoS One* 16 (12) (2021 December 20) e0261187, <https://doi.org/10.1371/journal.pone.0261187>.